Tunable Bandpass Filter Using Distributed MEMS Transmission Lines

B. Lakshminarayanan and T. Weller
Center for Wireless and Microwave Information Systems, University of South Florida, Tampa 33620

ABSTRACT

This paper presents a two-state tunable RF MEMS bandpass filter operating at 16.5 and 22 GHz. The topology consists of coplanar waveguide sections that are periodically loaded with MEMS capacitors. The passband insertion loss and bandwidth are 2.3 dB and 11.5% at 16.5 GHz, and 3.3 dB and 16.5% at 22 GHz. The typical switching voltage is 45-50V.

I. INTRODUCTION

Tunable filters are integral components in a variety of radar and modern multi-band communication systems. Conventional tunable filters typically utilize YIG resonators, active resonators or varactors as the tuning element. Varactor-based tunable filters have relatively low Q values in the range of 2-3 [1], due to the high series resistance of the diodes. The use of Micro–Electro–Mechanical Systems (MEMS) RF elements, such as switches and variable capacitors, can lead to improved performance given the potential for lower loss and better linearity.

In this paper, a 0.1dB Chebyshev prototype bandpass filter is designed on quartz using $\lambda/2$ shunt open stubs and $\lambda/4$ connecting lines. The series and the shunt transmission lines are capacitively-loaded by periodically spaced discrete MEMS capacitors, similar to the distributed MEMS transmission line (DMTL). Experimental results for the filter indicate a tuning from 22GHz to 16.5GHz, translating to 27% tuning at 22GHz. The relative bandwidth of the filter in the upstate and the downstate is approximately 16.5% and 11.5%, respectively.

The design and fabrication of the filter are described in Section III. In Section IV, the results of a sensitivity analysis on the effect of missing MEMS capacitors within the filter topology are summarized. The final conclusions are presented in Section V.

II. BACKGROUND

The distributed MEMS transmission line, initially reported by Barker et al. [2], consists of a length of high impedance coplanar waveguide (CPW) that is capacitively loaded by periodic placement of discrete MEMS capacitors. DMTL lines were used in designing an X-band variable resonator, which forms an integral part in a distributed tunable filter. [3]. Periodically-loaded lines were used in a distributed filter design that is presented in [4]. The design was a three-pole capacitively-coupled filter operating at 20GHz with a 3.8% tuning range. The insertion loss and return loss in the pass band were approximately 3.6dB and 30dB, respectively.

A two pole bandpass filter using semi-lumped components is described in [5]. In this design, two tunable spiral inductors are separated by a $\lambda/4$ CPW series resonator. The filter was tuned from 4.2GHz to 3.7GHz with 42% bandwidth. A completely-lumped element filter design that utilizes MEMS switches is reported in [6]. In this work, two sets of MEMS switches are connected with inductive beams and are switched alternatively to results in a tunable filter. A tuning range from 12.5GHz to 7GHz was reported with approximately 2dB insertion loss and 10dB return loss in the pass band.

III. DESIGN AND FABRICATION

The bandpass filter presented herein consists of nine reactive elements: six open stubs that are $\lambda/2$ long and three series $\lambda/4$ long connecting lines between the open stubs (Figure 1). The open stub design is preferred over a short end $\lambda/4$ stub design because it is easier to DC bias the circuit using coaxial bias tees. The series connecting sections (unloaded Z_0~80Ω) are periodically loaded with three shunt capacitors, each spaced by 850μm. The shunt $\lambda/2$ stubs (unloaded Z_0~70Ω) utilize four capacitors with a separation of 350μm. The beams used for the capacitors in the series and shunt sections are approximately 755μm and 970μm long, respectively; the beam width is held constant at 35μm. The overall footprint of the filter is 8mm×4.7mm

0-7803-7695-1/03/$17.00 © 2003 IEEE

and a total of 33 capacitive bridges are used. The widths of the center conductor and the slot for the feed arc 300μm and 30μm, respectively.

The series DMTL section is required to be approximately λ/4 long at each design center frequency. For an unloaded line on quartz, the corresponding lengths would be 2220μm at 22GHz and (2200+741=) 2961μm at 16.5GHz. The phase shift required to emulate the additional length of 741μm at 16.5GHz is found to be approximately 20°. Equation (1) can also be used to calculate the phase shift as a function of the CPW line characteristic impedance [7]:

$$\Delta\phi = \left(\frac{\omega Z_0 \sqrt{\varepsilon_{eff}}}{c}\right)\cdot\left(\frac{1}{Z_{up}} - \frac{1}{Z_{dn}}\right) \qquad (1)$$

where ω, Z_{up}, and Z_{dn} are the frequency, unloaded and loaded impedance, respectively. Three capacitive bridges separated by 850μm provide the necessary variation in characteristic impedance and result in a 90° phase shift at each of the desired frequencies (22 GHz in the up-state and 16.5 GHz in the down-state). The upstate and the downstate values of each MEMS capacitor are approximately 0.07pF and 0.1pF, respectively.

The shunt open stubs are λ/2 long at each design center frequency (5942μm at 16.5GHz; 4456μm at 22GHz). The length difference translates to a 44° phase difference at 16.5GHz. In this case, four capacitive bridges separated by 350μm are used. The upstate and the downstate capacitance for these capacitors are approximately 0.2 and 0.4pF, respectively. The higher capacitance values, relative to those used in the series sections, are used for two reasons: to reduce the size of the filter by increasing the loading, and to reduce the number of required bridges. It was also found that the increased distributed loading yields a better response than that obtained with a comparable design using shunt stubs that are terminated in large, single capacitors for length reduction.

Table 1 gives the capacitance values for the series and shunt sections. In order to design low capacitance ratios that are feasible to fabricate, MIM capacitors are used in series with the MEM bridges [9]. The MIM capacitors are placed 40-50μm away from each MEMS capacitor (Figure 2).

The starting values for the admittances of the shunt stubs were calculated using equations given in [8]. The final values of the admittances were found by circuit level simulation, after accounting for parasitics extracted via numerical EM simulation. Full-wave simulations were performed using ADS Momentum™. The parasitic effects due to the cross and the tee-junction discontinuities required the length of the shunt and series sections to be adjusted.

Table 1 - Capacitance values for the series λ/4 sections and the open λ/2 stubs in the upstate and downstate.

	C_{up} [pF]	C_{down} [pF]
Series λ/4 sections	0.07	0.1
Shunt λ/2 sections	0.2	0.4

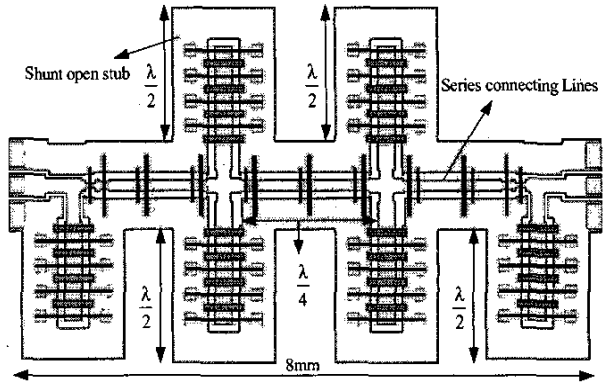

Figure 1- Schematic of the bandpass filter. The series connecting lines are λ/4 long and the shunt open stubs are λ/2 long at the design frequencies.

The filter is fabricated on a 480μm thick quartz substrate (ε_r=3.7, tanδ=0.0004). The fabrication steps are as follows:

- A 0.5μm thick Si_3N_4 is blanket deposited using RF magnetron sputtering to improve the adhesion of metal lines on the quartz. Alternatively, a thin Cr layer can be used but this approach requires etching in subsequent fabrication steps.
- Lift–off processing is used to define metal lines to a thickness of 1μm (Cr/Ag/Cr).
- A 3μm thick photosensitive cyclotene™ polymer (ε_r=2.7) is used to form a MIM capacitor dielectric layer.
- A 0.5μm thick Si_3N_4 is deposited using RF magnetron sputtering.
- Contact pads (0.2μm thick) comprised of Cr/Au are formed using liftoff processing for RF probing.
- Pedestal areas are patterned with photoresist and a 3μm thick cyclotene™ polymer is used to form the posts.
- A 0.8μm thick Al layer is sputtered on top the sacrificial photoresist layer and subsequently etched to form the capacitor beam geometry.

- The sacrificial photoresist is removed and critical point drying is used to release the MEMS capacitors.

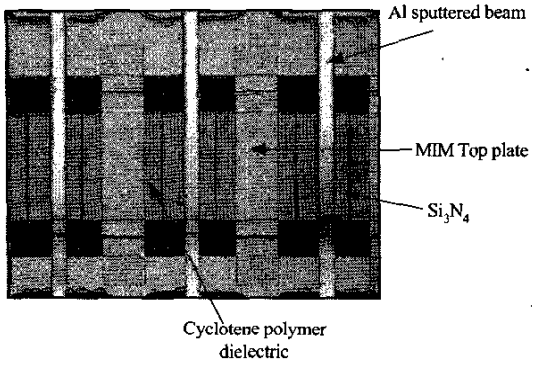

Figure 2: Microphotograph of the fabricated structure.

III. EXPERIMENTAL RESULTS

Measurements were performed from 5–30GHz using a Wiltron 360B vector network analyzer and 250μm pitch GGB microwave probes. A Thru–Reflect–Line (TRL) calibration was performed using calibration standards fabricated on the wafer. A high voltage bias tee was used to supply voltage through the RF probe to avoid damaging the VNA test ports. Typical actuation voltage of the beams is approximately 45-50V.

Figure 3 shows the comparison of S11 [dB] between the measured and simulated filter response in the upstate and the downstate. The measured response in the upstate has S11 < -19dB and the measured S11 in the downstate is less than -30dB. Figure 4 shows the comparison of S21 [dB] between the measured and simulated data in the upstate and the downstate. The measured data shows a maximum S21 of -3.3dB in the passband (20.4-24GHz) in the upstate and S21 is approximately -2.3dB in the passband (15.7-17.8GHz).

The relative bandwidth of the filter in the upstate is approximately 16.5% (20.4-24GHz) and the out of band rejection is better than 25dB over the measured frequency range. The measured data shows a larger bandwidth and higher insertion loss when compared to the simulation results for both states. The increased bandwidth is attributed to fabrication tolerance, resulting in a higher capacitance of the MEM bridges. The higher insertion loss may be due to the resistance of the bridges (not accounted for in the simulations).

The measured and the modeled filter results exhibit a spurious response above 25GHz that is associated with the $2\omega_0$ passband characteristic. The relative bandwidth of the filter is approximately 11.5%. The absolute bandwidth in the upstate and downstate is approximately 3.6GHz and 2.8GHz, respectively.

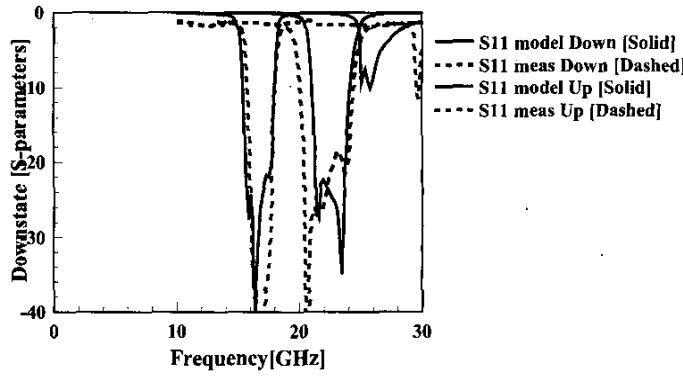

Figure 3: Comparison of S11 in the upstate and downstate between measured data and simulations. Solid lines represent EM simulation data and dashed lines represent measured data.

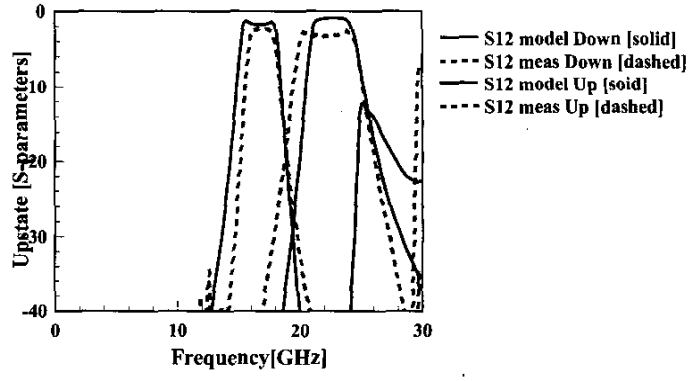

Figure 4: Comparison of S21 in the upstate and downstate between measured data and simulations. Solid lines represent EM simulation data and dashed lines represent measured data.

III. SENSITIVITY ANALYSIS

The filter presented herein utilizes 33 capacitive MEMS bridges. One or more bridges can fail during fabrication due to poor adhesion of the beams to the posts, or due to stress build-up in the beam that can lead to eventual breaking. In order to study the impact of damaged or missing beams, the filter was simulated at the circuit level with one or more beams being removed.

Figure 4 shows a comparison of S11 in the upstate when one or two beams from each of the series λ/4 sections are removed. In the optimal design, the series section includes three capacitive bridges. With the center capacitive beam being removed, S11 increased from -25dB to -9dB in the passband, and the passband shifted higher in frequency by approximately 8.1%. With two beams removed from the design, the response shifted higher in frequency by 8.6% relative to the optimal design. The shape of the passband and the out of band rejection was not greatly affected. The simulated results therefore predict a degradation in performance (~9% frequency shift) due to either of these two failure conditions. The design tolerance can be attributed to a low upstate capacitance (0.07pF) for the series section. The filter response in the downstate (at 16GHz) yields similar trends when compared with the upstate results but frequency shift was lower (~5%).

The shunt section, however, is more sensitive to beam failures due to the higher down state capacitance. The absence of one beam from each stub can shift the frequency by as much as 22 % in the upstate and by 24% in the downstate.

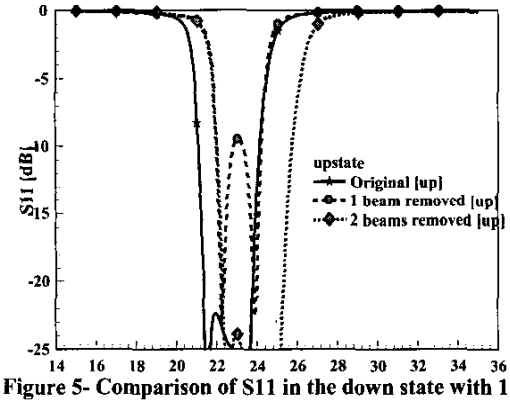

Figure 5- Comparison of S11 in the down state with 1 and 2 beams missing from the series λ/4 sections of the filter.

IV. SUMMARY

In this paper, a tunable CPW bandpass filter on quartz that utilizes DMTL series and shunt sections is presented. The tuning range of the filter is approximately 27% at 22GHz. Measured S21 in the passband for the upstate and downstate is approximately 3.3dB and 2.3dB, respectively. The relative bandwidth of the filter is 16.5% and 11.5% at 22 GHz and 16.5 GHz, respectively. Full wave simulation has been used to account for the parasitics associated with the tee- and cross-junctions. A sensitivity study on the filter response with respect to damaged MEMS capacitors in the series sections indicates <10% frequency shift when one or more beams is removed, but up to 25 % frequency shift if one beam is removed from each shunt stub.

ACKNOWLEGDEMENTS

The authors would like to thank Saravana P. Natarajan and Rajsekhar Poppuri for their help with Si_3N_4 and Aluminum sputtering. This work was supported by The National Science Foundation, grant number ECS-9875235. Partial support of this work was also provided by the USF Center for Ocean Technology.

REFERENCES

[1]. P. Blondy et al., "Applications of RF MEMS to Tunable Filters and Matching Networks," CAS 2001 Proceedings, Semiconductor Conference, vol. 1, 2001, pp. 111-116.

[2]. Scott Barker and Gabriel Rebeiz, "Distributed True–Time Delay Phase Shifters and Wide–Band Switches," IEEE Trans. MTT, vol. 46, no. 11, pp. 1881-1889, Nov 1998.

[3]. J.B. Muldavin and Gabriel Rebeiz, "X-band Tunable MEMS Resonators," 2000 Topical Meeting on Silicon Monolithic Integrated Circuits in RF systems, pp. 116-118.

[4]. Yu Liu, Andrea Borgioli et al., "Distributed MEMS Transmission Lines For Tunable Filter Applications," , Int'l Journal of RF and Microwave CAE, vol.11, pp. 254-260, 2001.

[5]. T. Ketterl, "Fabrication and Characterization of Micromachined Microfluidic Channels and Tunable Microwave Filters," Master's Thesis, University of South Florida, pp. 22, August 2000.

[6]. Dimitrios Peroulis, Sergio Pacheco, Kamal Sarabandi, and Linda P.B. Katehi, "MEMS Devices for High Isolation Switching and Tunable Filtering," 2000 IEEE MTT-S, vol. 2, pp. 1217-1220.

[7]. Joseph S. Hayden and Gabriel Rebeiz, "Low-loss cascadable MEMS Distributed X-band Phase Shifters," IEEE Microwave and Guided Wave Letters, vol. 10, no. 4, pp. 142-144, Apr 2000.

[8]. G. Matthaei, L. Young, and E.M.T Jones, Microwave Filters, Impedance-Matching Networks, and Coupling Structures, Artech House, New Jersey, 1980.

[9]. Andreas Borgioli, et al., "K–Band 3–bit Low – Loss Distributed MEMS Phase Shifter," IEEE Microwave and Guided Wave Letters, vol. 10, no. 10, pp. 415-417, Oct 2000.